Published in final edited form as:
Neurobiol Dis. 2009 April ; 34(1): 155–162.

Redox susceptibility of SOD1 mutants is associated with the differential response to CCS over-expression in vivo

Marjatta Son[*], **Qiao Fu**[*,#], **Krishna Puttaparthi**, **Christina M. Matthews**, and **Jeffrey L. Elliott**
Department of Neurology, University of Texas, Southwestern Medical Center, Dallas, Texas 75390

Abstract

Over-expression of CCS in G93A SOD1 mice accelerates neurological disease and enhances mitochondrial pathology. We studied the effect of CCS over-expression in transgenic mice expressing G37R, G86R or L126Z SOD1 mutations in order to understand factors which influence mitochondrial dysfunction. Over-expression of CCS markedly decreased survival and produced mitochondrial vacuolation in G37R SOD1 mice but not in G86R or L126Z SOD1 mice. Moreover, CCS/G37R SOD1 spinal cord showed specific reductions in mitochondrial complex IV subunits consistent with an isolated COX deficiency, while no such reductions were detected in CCS/G86R or CCS/L126Z SOD1 mice. CCS over-expression increased the ratio of reduced to oxidized SOD1 monomers in the spinal cords of G37R SOD1 as well as G93A SOD1 mice, but did not influence the redox state of G86R or L126Z SOD1 monomers. The effects of CCS on disease are SOD1 mutation dependent and correlate with SOD1 redox susceptibility.

Keywords

Amyotrophic Lateral Sclerosis; mitochondria; cytochrome c oxidase; transgenic; motor neuron; paralysis

There is increasing evidence that mitochondrial dysfunction may be important in the pathogenesis of familial amyotrophic lateral sclerosis (FALS) related to Cu, Zn superoxide dismutase (SOD1) mutations (Manfredi and Xu, 2005, Martin et al., 2007). Mitochondrial pathology, characterized by vacuolization, is a principal finding in G93A SOD1 transgenic mice that develop motor weakness (Dal Canto and Gurney, 1994). SOD1 has been detected within mitochondria raising the possibility of a direct toxic effect of G93A SOD1 on mitochondrial function (Okado-Matsumoto and Fridovich, 2001, Vijayvergiya et al., 2005). Copper chaperone for SOD1 (CCS) over-expression in G93A SOD1 mice increases mutant SOD1 levels within mitochondria, greatly accelerating disease course and enhancing mitochondrial vacuolar pathology (Son et al., 2007). Spinal cords from dual CCS/G93A SOD1 mice manifest isolated cytochrome *c* oxidase (COX) deficiency, which may underlie a substantial part of the mitochondrial cytopathy (Son et al., 2008).

Corresponding author: Jeffrey L. Elliott, Department of Neurology, University of Texas, Southwestern Medical Center, Dallas, Texas 75390, Phone: 214-645-6242, Fax: 214-645-6238, jeffrey.elliott@utsouthwestern.edu.
[*]Contributed equally to this paper
[#]Current Address: Rehabilitation Center, Hainan Provincial People's Hospital, Haikou, Hainan 570311, P.R. China

Although G93A SOD1 likely impacts mitochondrial function, in vivo evidence of direct mitochondrial toxicity for other SOD1 mutations is less complete. Sub-cellular fractionation studies have confirmed that other SOD1 mutants, including G37R, G85R, H46R/H48Q or L126Z SOD1, also accumulate with mitochondria and thus are capable of directly altering mitochondrial function (Liu et al., 2004, Deng et al., 2006). However, mitochondrial pathology varies greatly among transgenic mouse lines harboring different SOD1 mutations, possibly reflecting varied degrees of mitochondrial involvement in the disease process. Transgenic mice expressing G37R SOD1 develop marked mitochondrial vacuolar pathology, while L126Z, G85R (G86R in mouse), or H46R/H48Q SOD1 mice show little or no mitochondrial pathology (Wong et al., 1995, Bruijn et al., 1997, Wang et al., 2002, Wang et al., 2005). The basis for this difference among the transgenic lines is not well understood. Steady state levels of G93A SOD1 and G37R SOD1 within spinal cord are several fold higher than levels of G85R or L126Z SOD1, suggesting that mutant SOD1 protein overloading may lead to mitochondrial dysfunction (Bergemalm et al., 2006). However, because G37R SOD1 and H46R/H48Q SOD1 mice express similar high steady state SOD1 levels yet manifest different pathologies, factors other than protein loading influence the extent of mitochondrial pathology (Wang et al., 2002). SOD1 mutants differ in important biochemical parameters including copper binding, disulfide bond formation, or aggregation potential that may affect SOD1 structure and its ability to interact with other proteins which would promote mitochondrial toxicity (Furukawa and O'Halloran T, 2005, Krishnan et al., 2006, Wang et al., 2007, Vande Velde et al., 2008). We therefore crossed CCS transgenic mice with mice expressing various SOD1 mutations to better understand factors which influence mitochondrial pathology. CCS/G37R SOD1 mice show marked acceleration of neurological disease and enhancement of mitochondrial pathology. In contrast, CCS/L126Z SOD1 or CCS/G86R SOD1 mice show no such acceleration, manifesting a disease course indistinguishable from L126Z SOD1 or G86R SOD1 mice. The effect of CCS over-expression in accelerating disease is dependent on the specific SOD1 mutation and suggests that SOD1 interactions with other proteins may vary among differing SOD1 mutants.

Material and Methods

Transgenic mouse lines

G37R SOD1 (BL6SJL xC3H/HeJ) and L126Z SOD1(C57BL/6J xC3/HeJF1) transgenic mouse lines have been well characterized (Wong et al., 1995, Wang et al., 2005). Transgenic mice expressing a G86R SOD1 mutation in the endogenous genomic mouse SOD1 gene (Tg (Sod1*G86R)M1Jwg) were obtained from the Jackson Laboratory (Bar Harbor, ME). The characterization of G86R SOD1 mice (FVB/N) has been published (Ripps et al., 1995, Morrison et al., 1998). Low copy number human G93A SOD1 mice (B6SJL-TgNSOD1-G93A;Gur dl JR2300) were originally obtained from the Jackson Laboratory. The generation and characterization of CCS transgenic mice (line 17;B6SJLF1) has been described (Son et al., 2007). Line 17 CCS transgenic mice were crossed to either G37R, G86R, L126Z or G93A SOD1 mice to obtain CCS/SOD1 transgenic mice as previously described. Specific genotypes were identified by PCR on tail DNA. Animals unable to correct posture when placed on side were considered end stage for survival analysis (Puttaparthi et al., 2002). All animal protocols were approved by our university's Institutional Animal Care and Research Advisory Committee in compliance with National Institutes of Health guidelines.

Immunohistochemistry

Mice were overdosed with pentobarbital (250mg/kg, i. p.) and perfused transcardially with PBS followed by 4% paraformaldehyde. Spinal cords were post-fixed, sectioned, stained and viewed as previously described (Puttaparthi and Elliott, 2005, Son et al., 2007). In brief, spinal cord sections were pretreated for 2 hours with 5% normal goat serum and 0.1% Triton X-100 and then incubated overnight at 4°C with primary antibodies: mouse anti COX1 subunit,

16μg/ml, (clone ID6, Molecular Probes, Inc., Eugene, OR) or rabbit anti-ubiquitin, 1/1000 (Dako, Carpenteria, CA). Next day, the sections were washed, incubated for one hour at room temperature with secondary antibody: goat anti-mouse IgG labeled with Alexa Flour 488, 10μg/ml, or with goat anti-rabbit IgG labeled with Alexa Fluor 555, 10μg/ml (Molecular Probes, Eugene, OR). Next, they were counterstained by incubating for one minute with DAPI, 1/1000, (Molecular Probes). The sections were washed and mounted with Gel/mount (Biomed Corp., Foster City, CA). Slides were viewed with an E800 fluorescent microscope (Nikon Instruments Inc).

Electron microscopy

Anesthetized mice were perfused with PBS followed by 2% Glutaraldehyde in PBS. The dissected tissues were post-fixed in 2% glutaraldehyde in PBS. Routine Electron Microscopy processing was performed. Tissues were rinsed in 3 changes of PBS, post-fixed in 1% Osmium Tetroxide for one hour, dehydrated in a series of graded alcohols, followed by infiltration of propylene oxide and Epon. The tissues were subsequently embedded in Eponate 12 (Ted Pella, Inc.) embedding media and polymerized overnight in a 60 °C oven. Thick sections (1.0μm) were stained with toluidine blue and examined by light microscopy. Ultra thin sections (60-90 nm) were stained with Uranyl Acetate and Lead Citrate and examined on a Hitachi 7500 Electron Microscope.

Western Blot Analysis

Anesthetized mice were perfused transcardially with PBS. For Western Blots, the dissected tissues were homogenized in 20mM Tris-HCl, pH 7.5, 1 mM EDTA, 0.5% TritonX -100 (Sigma, St. Louis, MO). Mitochondria were isolated from dissected spinal cords using a mitochondrial isolation kit (Sigma). The protein concentrations were determined by BCA protein assay (Thermo Scientific, Rockford, IL). Samples were separated on 4-20% Tris-HCl (SDS-PAGE) gels and transferred to polyvinylidene difluoride membranes (PVDF). The experiments were performed using the following primary antibodies: sheep anti SOD1, 1/1600 (Calbiochem, EMD Biosciences, Inc. La Jolla, CA), rabbit anti SOD1, 0.2μg/ml (Stressgen Biotechnologies, Inc., Victoria, Canada), rabbit anti CCS, 0.1μg/ml (FL-274 Santa Cruz, Biotechnology, Inc., Santa Cruz, CA), mouse anti-COX1 subunit, 1ug/ml (clone 1D6) and mouse anti-COX5b subunit, 1μg/ml (clone 16H12) (Molecular Probes, Inc. Eugene, OR), mouse anti MS105 Complex I subunit 20kDA, 0.5μg/ml, mouse anti MS204 Complex II subunit 70kDa, 0.1μg/ml, mouse anti MS303 Complex III subunit core 1, 0.5 μg/ml, and mouse anti MS2503 Complex V subunit β, 0.5 μg/ml (MitoSciences, Eugene OR), and rabbit anti actin, 1μg/ml (Sigma). Secondary antibodies were Alkaline Phosphatase conjugated polyclonal antibodies 0.08 μg/ml (Santa Cruz Biotechnology). The immuno-reactive signals were detected by Lumi-Phos WB substrate (Thermo Scientific) and quantified by using ChemiDoc XRS Imaging system (BIO-RAD, Hercules, CA).

SOD1 disulfide analysis by IAM

SOD1 disulfide analysis was performed as previously described with slight modification (Jonsson et al., 2006, Proescher et al., 2008). Anesthetized mice were perfused transcardially with 100mM iodoacetamide (IAM) in PBS (BIO-RAD). Tissues were homogenized in buffer containing 50 mM Hepes/2.5%SDS/0.1 mM EDTA (pH 7.2) with 100 mM IAM, and homogenates were incubated at 37°C for 30 minutes. The protein concentrations were determined by BCA protein assay (Thermo Scientific). For SDS-PAGE, the samples were treated with Laemmli sample buffer (BIO-RAD) either without or with 3.7% β-mercaptoethanol. Only the reduced samples were boiled prior to electrophoresis on 15% Tris–HCl gels (SDS-PAGE). Prior to transfer onto PVDF membranes the proteins were subjected

to in-gel reduction by incubating two times for 10 min each in transfer buffer containing 2% β-mercaptoethanol to increase antibody recognition of disulfide-oxidized SOD1.

Results

The effect of CCS over-expression is SOD1 mutation dependent

In order to determine whether the effects of CCS on SOD1 disease were applicable to all SOD1 mutants or rather mutation specific, we crossed transgenic mice over-expressing CCS protein with lines expressing various SOD1 mutations and then observed changes in the disease course. Over-expression of CCS protein in G37R SOD1 mice markedly accelerated onset of neurological disease and impacted survival. By 10 days of age, CCS/G37R SOD1 mice develop a neurological disorder characterized by spasticity with extensor posturing, tremor and ataxia that is clinically similar to the phenotype of CCS/G93A SOD1 mice. CCS/G37R SOD1 mice then go on to manifest progressive limb paresis over the next two weeks while G37R SOD1 mice remain neurologically normal during this time period. Due to their severe neurological disease, CCS/G37R SOD1 mice show about 90% decline in survival compared to G37R SOD1 with a mean survival of 32 days versus 270 days (Fig. 1A). Thus CCS over-expression markedly accelerates disease in G37R SOD1 mice as it does in G93A SOD1 mice. In contrast, CCS/G86R SOD1 and CCS/L126Z SOD1 mice show no significant change in survival compared to G86R SOD1 or L126Z SOD1 mice respectively (Fig. 1B and C). CCS/L126Z SOD1 mice have a mean survival of 230 ± 5 days compared to 230 ± 4 days for L126Z SOD1 mice. CCS/G86R SOD1 mice have mean survival 115 ± 6 days compared to 113 ± 4 days for G86R SOD1 mice. In addition, there appeared to be no significant change in onset or disease severity in G86R or L126Z mice in the setting of CCS over-expression (data not shown). Western blot analysis confirmed that CCS levels were similar among the differing dual genotypes (Fig. 1D). Overall, these results indicate that the effect of CCS in accelerating disease in vivo is SOD1 mutation dependent. Interestingly, we did not observe any intermediate effect of CCS over-expression on the disease phenotype suggesting that the CCS effect is all or none.

CCS enhances mitochondrial pathology in G37R SOD1 mice but not in G86R SOD1 or L126Z SOD1 mice

We next investigated the pathology within spinal cords of the various mutant SOD1 lines over–expressing CCS protein. By three weeks of age, CCS/G37R SOD1 mice already show marked vacuolar pathology within ventral horn motor neurons (Fig. 2A). Such vacuoles are not observed in age matched G37R SOD1 littermates (Fig. 2B) or in three week old CCS/L126Z SOD1 (Fig. 2C) or CCS/G86R SOD1 mice (data not shown). Electron microscopy confirmed that these vacuolar structures are abnormal mitochondria (Fig. 2D and E). These mitochondria in CCS/G37R SOD1 mice appeared to be in differing stages of vacuolization that is characterized by disruption of the cristae and swelling with relative preservation of the outer membrane. In contrast, mitochondrial morphology in three week old CCS/L126Z SOD1 mice appears normal (Fig. 2F). Immuno-fluorescence studies using antibodies directed against a mitochondrially encoded subunit of complex IV of the mitochondrial respiratory chain, cytochrome c oxidase (COX) subunit 1, revealed markedly weaker immuno-staining in the ventral horn motor neurons from 3 week old CCS/G37R SOD1 mice compared to age-matched G37R SOD1 controls (Fig. 2G and H). In addition, the COX1 staining has a clumped rather than a normal punctuate pattern observed in young G37R SOD1 mice. In contrast, three week old CCS/L126SOD1 and CCS/G86R SOD1 mice show normal punctuate COX1 staining patterns that are similar to young G37R SOD1 mice and other controls (Fig. 2I and J). These results indicate that enhanced mitochondrial pathology accompanies the accelerated motor phenotype seen in G37R SOD1 mice over-expressing CCS. In contrast, CCS over–expression in L126Z or G86R SOD1 mice does not accelerate mitochondrial pathology.

Isolated complex IV deficiency occurs with disease acceleration

The abnormalities in COX1 immuno-staining in CCS/G37R SOD1 mouse spinal cord prompted us to ask whether these mice show changes in levels for protein subunits of other mitochondrial OXPHOS complexes or rather manifest an isolated cytochrome c oxidase deficiency. Immuno-blots performed on mitochondrial enriched fractions from the spinal cords of young G37R SOD1 mice or CCS/G37R SOD1 mice demonstrate a significant reduction in levels for COX1, a mitochondrially encoded subunit of cytochrome c oxidase (complex IV) and COX5b, a nuclear encoded subunit of complex IV, for the CCS/G37R SOD1 mice (Fig. 3A). However, CCS/G37R SOD1 spinal cords show no decline compared to G37R SOD1 spinal cord in levels of NDUF8, a nuclear encoded complex I subunit; Fp70, a nuclear encoded complex II subunit; core 1, a nuclear encoded complex III subunit; or ATPase β, a nuclear encoded complex V subunit. These results indicate that CCS/G37R SOD1 mice manifest an isolated deficiency of complex IV subunits within spinal cord. In contrast, CCS/L126Z SOD1 mice and L126Z SOD1 mice show comparable levels of COX1 and COX5b subunits within spinal cord (Fig. 3B). Similarly, CCS/G86R SOD1 mice show no loss of COX1 and COX 5b subunit steady state levels compared to G86R SOD1 mice (Fig. 3B). Thus, the reduction of complex IV subunits correlates with the accelerated neurological phenotype observed in G37R SOD1 mice over-expressing CCS, while complex IV levels are preserved in the spinal cords of CCS/L126Z or CCS/G86R SOD1 mice that do not manifest disease acceleration. This strong association between complex IV deficits and motor phenotype is consistent with a causal relationship between mutant SOD1 induced COX deficiency and the disease state.

SOD1 aggregation in the setting of CCS over-expression

The presence of SOD1 positive aggregates is a pathologic hallmark of disease in mutant SOD1 transgenic mice and hypothesized to be an essential part of mutant SOD1 toxicity. However, we have previously shown that CCS/G93A SOD1 mice exhibit severe neurological deficits without accumulating SOD1 aggregates (Son et al., 2007, Proescher et al., 2008). We therefore wished to determine the effect of CCS over-expression on aggregation in end-stage transgenic mice harboring differing SOD1 mutations (Fig. 4). Western blots of spinal cord homogenates from paralyzed G37R or G93A SOD1 mice probed with anti-SOD1 show a well recognized pattern of high molecular weight SOD1 positive complexes (HMWPCs)(Fig. 4A). However, such complexes are not observed in spinal cords from paralyzed CCS/G37R SOD1 or CCS/G93A SOD1 mice. The single high molecular weight SOD1 positive band (about 50kD) present is also observed in spinal cords from CCS/WT SOD1 mice that do not manifest a neurological phenotype (Son et al., 2007). For paralyzed G86R and L126Z SOD1 mice, levels of SOD1 positive complexes within spinal cord are unchanged in the setting of CCS over-expression (Fig. 4A). On immuno-staining spinal cord sections with ubiquitin antibodies, we could detect abundant ubiquitin positive inclusions within neurons and the neuropil of weak G37R SOD1 mice but did not observe these ubiquitin positive inclusions within spinal cord of weak CCS/G37R SOD1 mice (Fig. 4B and C). Ubiquitin positive inclusions were present in weak CCS/G86R SOD1 and CCS/L126Z SOD1 mice at levels comparable to those seen in weak G86R SOD1 or L126Z SOD1 mice (data not shown). These results indicate that G37R SOD1 induced disease in the context of CCS over-expression, like G93A SOD1 induced disease, may occur without prominent signs of SOD1 aggregation as manifested by SOD1 positive HMWPCs or ubiquitin positive inclusions.

SOD1 redox state and disease acceleration

The finding that CCS over-expression accelerated disease in SOD1 transgenic mice with only certain mutations led us to investigate SOD1 biochemical parameters potentially influenced by CCS. Because SOD1 contains two cysteine residues (C57 and C146) that can form an intra-molecular disulfide bond, SOD1 monomers may exist in either a reduced or oxidized state that

affects its function, stability and its sub-cellular localization. We therefore assessed the redox state of the differing SOD1 mutants with or without CCS over-expression in spinal cord extracts by using an iodacetamide (IAM) based assay where disulfide-oxidized and disulfide reduced SOD1 are differentiated by non-reducing gel electrophoresis following thiol protection by IAM (Fig. 5). The G37R SOD1 monomer primarily exists in an oxidized form with only a small fraction found in the reduced form (Fig. 5A). However, in the presence of CCS over-expression, there is a shift toward a greater fraction of the G37R monomer being found in the reduced form. This pattern is similar to what is observed for G93A SOD1, in that CCS over-expression favors a shift toward the reduced form of the monomer but contrasts to what we have reported in mice transgenic for human wild type SOD1 where CCS over-expression favors the oxidized form (Proescher et al., 2008). For both G86R and L126Z SOD1 mutants, we observe that the monomer exists in a single form and is not altered in the setting of CCS over-expression. To determine the redox state of this single form of the SOD1 monomer, we analyzed IAM treated spinal cord samples from G86R SOD1, L126Z SOD1, CCS/G86R and CCS/L126Z dual mice under both non-reducing and reducing conditions (Fig. 5B). All samples showed a single SOD1 species present. Moreover, there was no difference in the SOD1 band position in the gel between samples that were native and those that were reduced indicating that G86R SOD1 and L126Z monomers exist largely in the reduced form. These IAM based assays indicate that SOD1 mutants in which the disease can be accelerated by CCS over-expression exist in both oxidized and reduced monomeric forms, while those SOD1 mutants whose disease course are unaffected by CCS appear to exist primarily in a single reduced monomeric form. Moreover, because CCS over-expression in vivo results in a shift toward an increased amount of reduced G37R or G93A SOD1 monomer as the disease state is accelerated, this correlation provides additional evidence that it is the reduced form of mutant SOD1 which represents the toxic moiety.

Discussion

CCS over-expression in G93A SOD1 transgenic mice results in the most marked acceleration of the disease course currently recognized (Son et al., 2007, Turner and Talbot, 2008). We therefore wished to learn whether CCS over-expression would affect disease course in transgenic mice harboring various other SOD1 mutants and our results indicate that the ability of CCS to accelerate disease is dependent on the SOD1 mutant. CCS over-expression worsens survival in G37R SOD1 mice by nearly 10 fold, a level comparable to that observed for CCS/G93A SOD1 mice. In contrast, CCS expression appears to have no effect on disease course in G86R SOD1 or L126Z SOD1 mice. To our knowledge, this is the first example of such a marked dichotomy related to modifiers of mutant SOD1 induced disease in vivo, and this finding has significant implications for understanding the pathogenesis of SOD1 related ALS. It indicates that changes in important known and possibly unknown disease modifiers may have significantly differing effects on the various SOD1 mutants in vivo. Because only certain SOD1 mutants may be affected by specific modifiers, the potential molecular pathways by which a mutant SOD1 produces disease may be quite distinct in one class of mutant compared to another. Therefore, specific therapeutic interventions may need to be targeted for the particular type of mutation.

Enhanced mitochondrial pathology, rather than increased SOD1 aggregation, appears to be a characteristic feature of CCS accelerated disease observed with both G37R and G93A SOD1 mutations and indicates that mitochondrial dysfunction likely plays a prominent role. Mitochondrial vacuolar pathology has been observed in end-stage G37R SOD1 mice and both high and low copy G93A SOD1 mice (Wong et al., 1995, Watanabe et al., 2001, Sasaki et al., 2004). We did not observe any accumulation of SOD1 positive high molecular weight protein complexes or ubiquitin positive inclusions in spinal cords of paralyzed CCS/G37R SOD1 mice demonstrating that such aggregates are not necessary for neurological disease related to G37R

SOD1. One potential clue of how mutant SOD1 (G37R or G93A) might produce mitochondrial dysfunction could be related to a key biochemical abnormality observed in spinal cords from G37R and G93A SOD1 mice (Kirkinezos et al., 2005, Son et al., 2008). Spinal cords from both CCS/G37R and CCS/G93A SOD1 mice manifest an isolated complex IV (COX) deficiency characterized by loss of both nuclear and mitochondrial encoded complex IV subunits (Son et al., 2008). This reduction in complex IV is not observed in either CCS/G86R or CCS/126Z SOD1 mice indicating that low COX levels are not an unspecific consequence of dual CCS and mutant SOD1 expression. Isolated COX deficiency perfectly correlates with mitochondrial pathology and motor deficits in a pattern consistent with a causative role.

Complex IV (COX), the terminal oxido-reductase in the mitochondrial respiratory chain, is composed of 10 nuclear encoded subunits, including COX5b, and three mitochondrially encoded subunits, COX1, COX2 and COX3, which form the catalytic core of the enzyme (Shoubridge, 2001). In addition, the assembly of individual structural subunits into a functional holo-enzyme also requires a host of nuclear encoded accessory factors. Isolated COX deficiency has been associated with only a limited number of molecular etiologies in mammalian cells, implicating specific pathways by which mutant SOD1 may cause complex IV defects. Functional losses of accessory proteins required for the incorporation of copper (COX17, SCO1, SCO2) or generation of heme a (COX10, COX15) in complex IV lead to its selective deficiency(Papadopoulou et al., 1999, Jaksch et al., 2000, Valnot et al., 2000, Takahashi et al., 2002, Antonicka et al., 2003a, Antonicka et al., 2003b, Diaz et al., 2005). It is reasonable to hypothesize that G37R SOD1 or G93A SOD1 may produce complex IV loss via disruption of any of these accessory COX pathways.

By accelerating disease course in CCS/G37R and CCS/G93A SOD1 mice but not in CCS/G86R and CCS/L126Z SOD1 mice, CCS over-expression must change a critical biochemical parameter within certain SOD1 mutations but not in others. Our results here suggest that one possible explanation is provided by the SOD1 redox state. Wild type human SOD1 contains two cysteine residues (C57 and C146) that form intramolecular disulfide bonds and allow the SOD1 monomer to exist in either an oxidized or reduced form within CNS tissues. The C57 residue also allows for a transitory disulfide bond interaction between SOD1 and CCS that facilitates SOD1 maturation and oxidation (Lamb et al., 2001, Brown et al., 2004). As predicted by in vitro assays, CCS over-expression in vivo results in a marked change of the SOD1 redox state, where virtually all of the wild type SOD1 monomer is shifted to the oxidized form (Proescher et al., 2008). In contrast, CCS over-expression increases the proportion of the reduced form of G37R and G93A SOD1, which, like wild type SOD1, can exist in both redox states. Conversely, G86R SOD1 and L126Z SOD1 exist virtually all in the reduced form (Jonsson et al., 2006). Thus, CCS over-expression in vivo cannot reduce G86R SOD1 and L126Z SOD1 further and consequently would not be predicted to alter disease course for these mutants.

The sub-cellular localization of SOD1 varies from one mutant to another and there is increasing evidence that the redox state of SOD1 affects the distribution of SOD1 in the different mitochondrial compartments. Wild type SOD1 and certain SOD1 mutants, like G93A, that exist in both redox states substantially localize to the mitochondrial intermembrane space (IMS), while SOD1 mutants that exist largely in the reduced state, like G85R, localize mainly to the cytoplasmic surface of the mitochondrial outer membrane (Sturtz et al., 2001, Inarrea et al., 2005, Vande Velde et al., 2008). In support of this idea, recent experiments have shown that loss of SOD1 cysteine residues (with the concomitant loss of their ability to be oxidized and form disulfide bonds) leads to poor mitochondrial localization of mutant SOD1 while having little impact on SOD1 aggregation potential (Karch and Borchelt, 2008, Kawamata and Manfredi, 2008). Moreover, while CCS over-expression serves to increase the mitochondrial sub-localization of some SOD1 mutants, like G93A, CCS has little impact on altering

mitochondrial localization of mutants like G85R (Son et al., 2007, Kawamata and Manfredi, 2008). Recent work has established the importance of a Mia40 disulfide relay system in the localization of proteins in the mitochondrial IMS including CCS and SOD1 (Reddehase et al., 2008). SOD1 mutants, such as G86R or L126Z, which are found fully in the reduced form, would not be expected to participate in this disulfide relay system.

The presence of an increased pool of reduced SOD1 within the IMS would likely have deleterious consequences for mitochondrial function. Increased amounts of G93A SOD1 within the mitochondrial IMS have been shown to significantly elevate levels of toxic reactive oxygen species (Goldsteins et al., 2008). Because G37R and G93A SOD1 are shifted toward the reduced form, these molecules would be able to interact inappropriately with other cysteine containing proteins in the IMS interfering with their normal function. Such interactions with cysteine containing COX accessory proteins may underlie the isolated COX deficiency observed in CCS/G37R SOD1 or CCS/G93A SOD1 mice and explain the profound mitochondrial dysfunction seen in vivo.

Acknowledgments

We would like to thank Dr. David Borchelt for the G37R and L126Z SOD1 transgenic mice. This work was supported by funding from the NINDS (R01NS055315), Muscular Dystrophy Association, The Horace C. Cabe Foundation, and The Judith and Jean Pape Adams Charitable Foundation

References

Antonicka H, Leary SC, Guercin GH, Agar JN, Horvath R, Kennaway NG, Harding CO, Jaksch M, Shoubridge EA. Mutations in COX10 result in a defect in mitochondrial heme A biosynthesis and account for multiple, early-onset clinical phenotypes associated with isolated COX deficiency. Hum Mol Genet 2003a;12:2693–2702. [PubMed: 12928484]

Antonicka H, Mattman A, Carlson CG, Glerum DM, Hoffbuhr KC, Leary SC, Kennaway NG, Shoubridge EA. Mutations in COX15 produce a defect in the mitochondrial heme biosynthetic pathway, causing early-onset fatal hypertrophic cardiomyopathy. Am J Hum Genet 2003b;72:101–114. [PubMed: 12474143]

Bergemalm D, Jonsson PA, Graffmo KS, Andersen PM, Brannstrom T, Rehnmark A, Marklund SL. Overloading of stable and exclusion of unstable human superoxide dismutase-1 variants in mitochondria of murine amyotrophic lateral sclerosis models. J Neurosci 2006;26:4147–4154. [PubMed: 16624935]

Brown NM, Torres AS, Doan PE, O'Halloran TV. Oxygen and the copper chaperone CCS regulate posttranslational activation of Cu,Zn superoxide dismutase. Proc Natl Acad Sci U S A 2004;101:5518–5523. [PubMed: 15064408]

Bruijn LI, Becher MW, Lee MK, Anderson KL, Jenkins NA, Copeland NG, Sisodia SS, Rothstein JD, Borchelt DR, Price DL, Cleveland DW. ALS-linked SOD1 mutant G85R mediates damage to astrocytes and promotes rapidly progressive disease with SOD1-containing inclusions. Neuron 1997;18:327–338. [PubMed: 9052802]

Dal Canto MC, Gurney ME. Development of central nervous system pathology in a murine transgenic model of human amyotrophic lateral sclerosis. Am J Pathol 1994;145:1271–1279. [PubMed: 7992831]

Deng HX, Shi Y, Furukawa Y, Zhai H, Fu R, Liu E, Gorrie GH, Khan MS, Hung WY, Bigio EH, Lukas T, Dal Canto MC, O'Halloran TV, Siddique T. Conversion to the amyotrophic lateral sclerosis phenotype is associated with intermolecular linked insoluble aggregates of SOD1 in mitochondria. Proc Natl Acad Sci U S A 2006;103:7142–7147. [PubMed: 16636275]

Diaz F, Thomas CK, Garcia S, Hernandez D, Moraes CT. Mice lacking COX10 in skeletal muscle recapitulate the phenotype of progressive mitochondrial myopathies associated with cytochrome c oxidase deficiency. Hum Mol Genet 2005;14:2737–2748. [PubMed: 16103131]

Furukawa Y, O'Halloran TV. Amyotrophic Lateral Sclerosis Mutations Have the Greatest Destabilizing Effect on the Apo- and Reduced Form of SOD1, Leading to Unfolding and Oxidative Aggregation. J Biol Chem 2005;280:17266–17274. [PubMed: 15691826]

Goldsteins G, Keksa-Goldsteine V, Ahtoniemi T, Jaronen M, Arens E, Akerman K, Chan PH, Koistinaho J. Deleterious role of superoxide dismutase in the mitochondrial intermembrane space. J Biol Chem 2008;283:8446–8452. [PubMed: 18171673]

Inarrea P, Moini H, Rettori D, Han D, Martinez J, Garcia I, Fernandez-Vizarra E, Iturralde M, Cadenas E. Redox activation of mitochondrial intermembrane space Cu,Zn-superoxide dismutase. Biochem J 2005;387:203–209. [PubMed: 15537389]

Jaksch M, Ogilvie I, Yao J, Kortenhaus G, Bresser HG, Gerbitz KD, Shoubridge EA. Mutations in SCO2 are associated with a distinct form of hypertrophic cardiomyopathy and cytochrome c oxidase deficiency. Hum Mol Genet 2000;9:795–801. [PubMed: 10749987]

Jonsson PA, Graffmo KS, Andersen PM, Brannstrom T, Lindberg M, Oliveberg M, Marklund SL. Disulphide-reduced superoxide dismutase-1 in CNS of transgenic amyotrophic lateral sclerosis models. Brain 2006;129:451–464. [PubMed: 16330499]

Karch CM, Borchelt DR. A limited role for disulfide cross-linking in the aggregation of mutant SOD1 linked to familial amyotrophic lateral sclerosis. J Biol Chem 2008;283:13528–13537. [PubMed: 18316367]

Kawamata H, Manfredi G. Different regulation of wild type and mutant Cu,Zn superoxide dismutase localization in mammalian mitochondria. Hum Mol Genet. 2008

Kirkinezos IG, Bacman SR, Hernandez D, Oca-Cossio J, Arias LJ, Perez-Pinzon MA, Bradley WG, Moraes CT. Cytochrome c association with the inner mitochondrial membrane is impaired in the CNS of G93A-SOD1 mice. J Neurosci 2005;25:164–172. [PubMed: 15634778]

Krishnan U, Son M, Rajendran B, Elliott JL. Novel Mutations that Enhance or Repress the Aggregation Potential of SOD1. Mol Cell Biochem 2006;287:201–211. [PubMed: 16583143]

Lamb AL, Torres AS, O'Halloran TV, Rosenzweig AC. Heterodimeric structure of superoxide dismutase in complex with its metallochaperone. Nat Struct Biol 2001;8:751–755. [PubMed: 11524675]

Liu J, Lillo C, Jonsson PA, Vande Velde C, Ward CM, Miller TM, Subramaniam JR, Rothstein JD, Marklund S, Andersen PM, Brannstrom T, Gredal O, Wong PC, Williams DS, Cleveland DW. Toxicity of familial ALS-linked SOD1 mutants from selective recruitment to spinal mitochondria. Neuron 2004;43:5–17. [PubMed: 15233913]

Manfredi G, Xu Z. Mitochondrial dysfunction and its role in motor neuron degeneration in ALS. Mitochondrion 2005;5:77–87. [PubMed: 16050975]

Martin LJ, Liu Z, Chen K, Price AC, Pan Y, Swaby JA, Golden WC. Motor neuron degeneration in amyotrophic lateral sclerosis mutant superoxide dismutase-1 transgenic mice: mechanisms of mitochondriopathy and cell death. J Comp Neurol 2007;500:20–46. [PubMed: 17099894]

Morrison BM, Janssen WG, Gordon JW, Morrison JH. Time course of neuropathology in the spinal cord of G86R superoxide dismutase transgenic mice. J Comp Neurol 1998;391:64–77. [PubMed: 9527542]

Okado-Matsumoto A, Fridovich I. Subcellular distribution of superoxide dismutases (SOD) in rat liver: Cu,Zn-SOD in mitochondria. J Biol Chem 2001;276:38388–38393. [PubMed: 11507097]

Papadopoulou LC, Sue CM, Davidson MM, Tanji K, Nishino I, Sadlock JE, Krishna S, Walker W, Selby J, Glerum DM, Coster RV, Lyon G, Scalais E, Lebel R, Kaplan P, Shanske S, De Vivo DC, Bonilla E, Hirano M, DiMauro S, Schon EA. Fatal infantile cardioencephalomyopathy with COX deficiency and mutations in SCO2, a COX assembly gene. Nat Genet 1999;23:333–337. [PubMed: 10545952]

Proescher JB, Son M, Elliott JL, Culotta VC. Biological effects of CCS in the absence of SOD1 enzyme activation: implications for disease in a mouse model for ALS. Hum Mol Genet 2008;17:1728–1737. [PubMed: 18337307]

Puttaparthi K, Elliott JL. Non-neuronal induction of immunoproteasome subunits in an ALS model: possible mediation by cytokines. Exp Neurol 2005;196:441–451. [PubMed: 16242125]

Puttaparthi K, Gitomer WL, Krishnan U, Son M, Rajendran B, Elliott JL. Disease progression in a transgenic model of familial amyotrophic lateral sclerosis is dependent on both neuronal and non-neuronal zinc binding proteins. J Neurosci 2002;22:8790–8796. [PubMed: 12388585]

Reddehase S, Grumbt B, Neupert W, Hell K. The Disulfide Relay System of Mitochondria Is Required for the Biogenesis of Mitochondrial Ccs1 and Sod1. J Mol Biol. 2008

Ripps ME, Huntley GW, Hof PR, Morrison JH, Gordon JW. Transgenic mice expressing an altered murine superoxide dismutase gene provide an animal model of amyotrophic lateral sclerosis. Proc Natl Acad Sci U S A 1995;92:689–693. [PubMed: 7846037]

Sasaki S, Warita H, Murakami T, Abe K, Iwata M. Ultrastructural study of mitochondria in the spinal cord of transgenic mice with a G93A mutant SOD1 gene. Acta Neuropathol (Berl) 2004;107:461–474. [PubMed: 15029445]

Shoubridge EA. Cytochrome c oxidase deficiency. Am J Med Genet 2001;106:46–52. [PubMed: 11579424]

Son M, Leary SC, Romain N, Pierrel F, Winge DR, Haller RG, Elliott JL. Isolated Cytochrome c Oxidase Deficiency in G93A SOD1 Mice Overexpressing CCS Protein. J Biol Chem 2008;283:12267–12275. [PubMed: 18334481]

Son M, Puttaparthi K, Kawamata H, Rajendran B, Boyer PJ, Manfredi G, Elliott JL. Overexpression of CCS in G93A-SOD1 mice leads to accelerated neurological deficits with severe mitochondrial pathology. Proc Natl Acad Sci U S A 2007;104:6072–6077. [PubMed: 17389365]

Sturtz LA, Diekert K, Jensen LT, Lill R, Culotta VC. A fraction of yeast Cu,Zn-superoxide dismutase and its metallochaperone, CCS, localize to the intermembrane space of mitochondria. A physiological role for SOD1 in guarding against mitochondrial oxidative damage. J Biol Chem 2001;276:38084–38089. [PubMed: 11500508]

Takahashi Y, Kako K, Kashiwabara S, Takehara A, Inada Y, Arai H, Nakada K, Kodama H, Hayashi J, Baba T, Munekata E. Mammalian copper chaperone Cox17p has an essential role in activation of cytochrome C oxidase and embryonic development. Mol Cell Biol 2002;22:7614–7621. [PubMed: 12370308]

Turner BJ, Talbot K. Transgenics, toxicity and therapeutics in rodent models of mutant SOD1-mediated familial ALS. Prog Neurobiol 2008;85:94–134. [PubMed: 18282652]

Valnot I, Osmond S, Gigarel N, Mehaye B, Amiel J, Cormier-Daire V, Munnich A, Bonnefont JP, Rustin P, Rotig A. Mutations of the SCO1 gene in mitochondrial cytochrome c oxidase deficiency with neonatal-onset hepatic failure and encephalopathy. Am J Hum Genet 2000;67:1104–1109. [PubMed: 11013136]

Vande Velde C, Miller TM, Cashman NR, Cleveland DW. Selective association of misfolded ALS-linked mutant SOD1 with the cytoplasmic face of mitochondria. Proc Natl Acad Sci U S A. 2008

Vijayvergiya C, Beal MF, Buck J, Manfredi G. Mutant superoxide dismutase 1 forms aggregates in the brain mitochondrial matrix of amyotrophic lateral sclerosis mice. J Neurosci 2005;25:2463–2470. [PubMed: 15758154]

Wang J, Caruano-Yzermans A, Rodriguez A, Scheurmann JP, Slunt HH, Cao X, Gitlin J, Hart PJ, Borchelt DR. Disease-associated mutations at copper ligand histidine residues of superoxide dismutase 1 diminish the binding of copper and compromise dimer stability. J Biol Chem 2007;282:345–352. [PubMed: 17092942]

Wang J, Xu G, Gonzales V, Coonfield M, Fromholt D, Copeland NG, Jenkins NA, Borchelt DR. Fibrillar inclusions and motor neuron degeneration in transgenic mice expressing superoxide dismutase 1 with a disrupted copper-binding site. Neurobiol Dis 2002;10:128–138. [PubMed: 12127151]

Wang J, Xu G, Li H, Gonzales V, Fromholt D, Karch C, Copeland NG, Jenkins NA, Borchelt DR. Somatodendritic accumulation of misfolded SOD1-L126Z in motor neurons mediates degeneration: alphaB-crystallin modulates aggregation. Hum Mol Genet 2005;14:2335–2347. [PubMed: 16000321]

Watanabe M, Dykes-Hoberg M, Culotta VC, Price DL, Wong PC, Rothstein JD. Histological evidence of protein aggregation in mutant SOD1 transgenic mice and in amyotrophic lateral sclerosis neural tissues. Neurobiol Dis 2001;8:933–941. [PubMed: 11741389]

Wong PC, Pardo CA, Borchelt DR, Lee MK, Copeland NG, Jenkins NA, Sisodia SS, Cleveland DW, Price DL. An adverse property of a familial ALS-linked SOD1 mutation causes motor neuron disease characterized by vacuolar degeneration of mitochondria. Neuron 1995;14:1105–1116. [PubMed: 7605627]

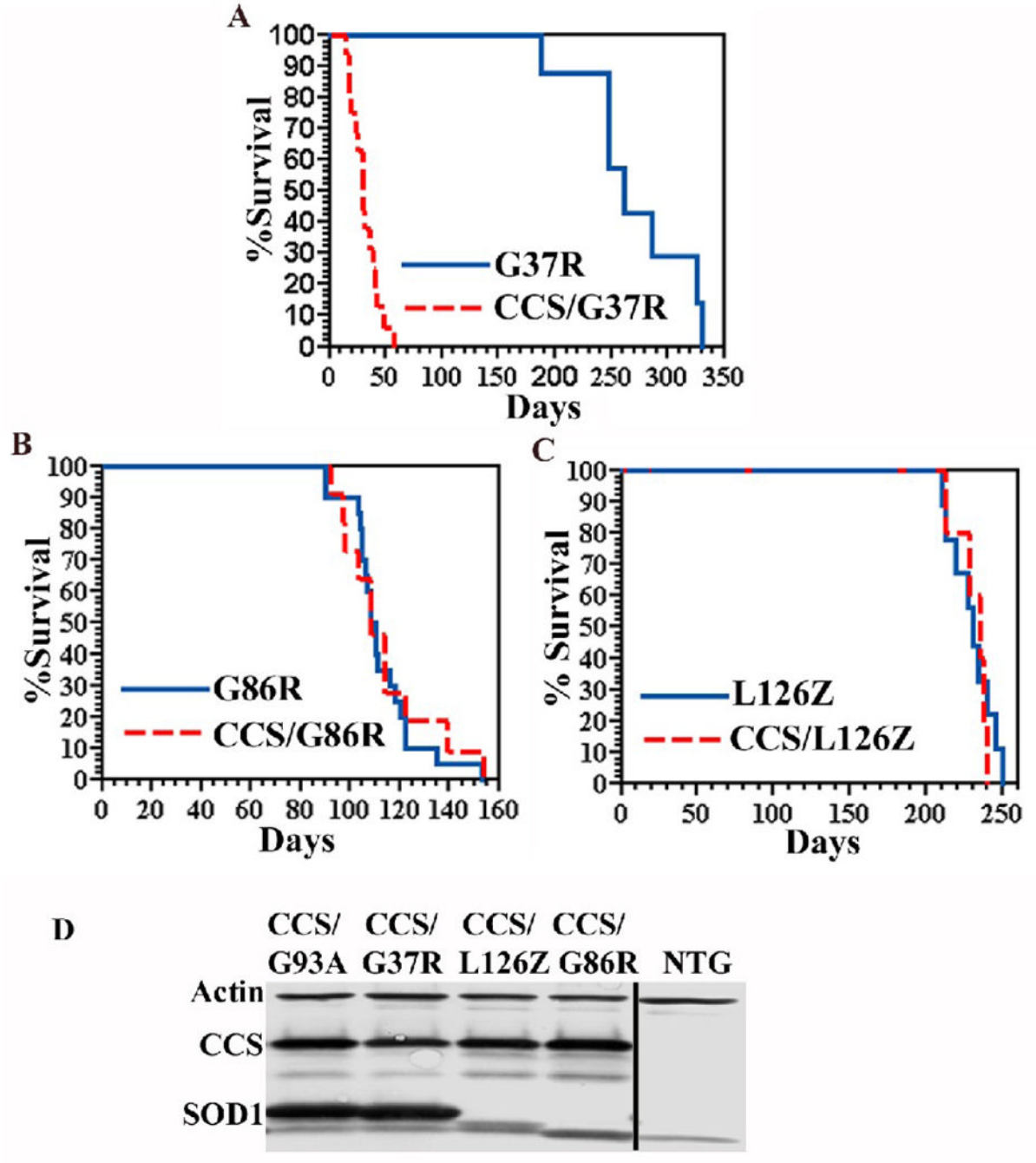

Fig. 1.

A-C. CCS over-expression greatly shortens the lifespan in G37R SOD1 but not in G86R SOD1 or L126Z SOD1 transgenic mice. Kaplan–Meier survival curves for A. CCS/G37R SOD1 mice (n=16) and G37R SOD1 mice (n=7); B. CCS/G86R SOD1 mice (n=11) and G86R SOD1 mice (n=18); C. CCS/L126Z mice (n=5) and L126Z SOD1 mice (n=9). The survival of CCS/G37R SOD1 mice is significantly shorter than that of G37R SOD1 mice (P<0.001; Log Rank Test). There is no difference in survival between CCS/G86R SOD1 mice and G86R SOD1 mice (P=.549; Log Rank Test) or between CCS/L126Z SOD1 mice and L126Z SOD1 mice (P =.775; Log Rank Test).

D. CCS expression is similar in differing dual transgenic line. Western blot analysis of spinal cord extracts from 3-4 week old mice (CCS/G93A SOD1, CCS/G37R SOD1, CCS/L126Z SOD1, CCS/86R SOD1 and non-transgenic (NTG) mice). 15μg of total protein was loaded per lane. Filter was probed with antibodies for CCS, SOD1 and actin (used as a loading control)

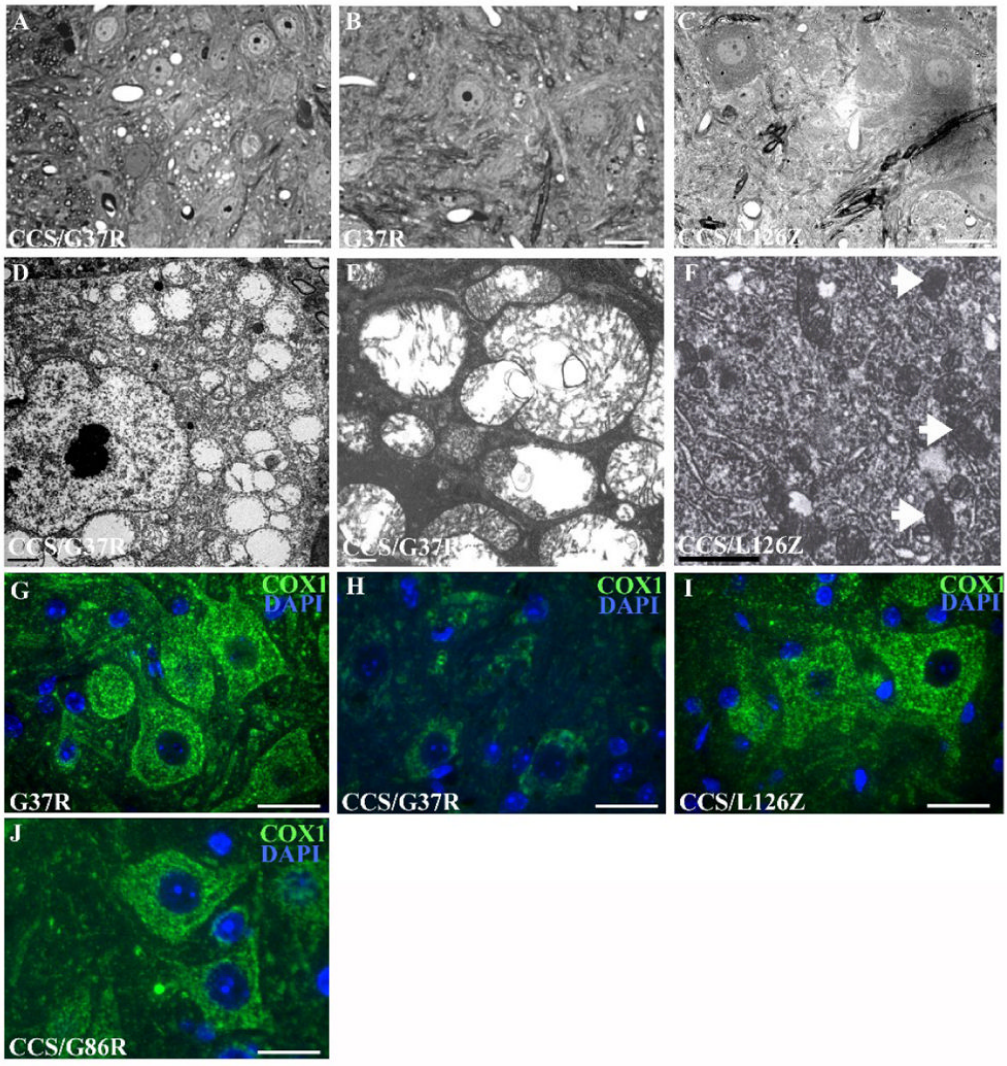

Fig. 2.

CCS over-expression enhances mitochondrial pathology in spinal cords of G37R SOD1 transgenic mice but not in L126Z SOD1 or G86R SOD1 mice.

Semi-thin toluidine blue stained plastic sections of lumbar spinal cord ventral horn of three week old (A) CCS/G37R SOD1 mice, (B) G37R SOD1, and (C) CCS/L126Z SOD1 mice. Extensive vacuolation is observed only in the ventral horn of CCS/G37R SOD1 mice.

Electron micrographs showing motor neurons in lumbar spinal cord of three week old (D and E) CCS/G37R SOD1, and (F) CCS/L126Z SOD1 mice. Large vacuolated mitochondria are seen within motor neurons of CCS/G37R SOD1 mice but not in motor neurons of CCS/L126Z SOD1 mice. Arrowheads indicate several normal appearing mitochondria.

Immuno-fluorescence performed on spinal cord ventral horn sections of three week old G37R SOD1 (G), CCS/G37R SOD1 (H), CCS/L126Z SOD1 (I), and CCS/G86R SOD1 mice (J), stained with COX1 (green), and counterstained with DAPI (blue).

CCS over-expression alters COX1 immuno-staining in G37R SOD1 spinal cord mitochondria. CCS/G37R SOD1 mice exhibit patchy COX1 distribution with overall decreased COX1 immuno-staining as compared to age-matched G37R SOD1 mice, which have normal COX1 staining pattern. Three week old CCS/L126Z SOD1 and CCS/G86R SOD1 mice show normal

COX1 immuno-staining patterns. Identical exposure times were used. Scale bars= 20 microns (A-C and G-J), 2 microns (D), 500nm (E) and 1 micron (F).

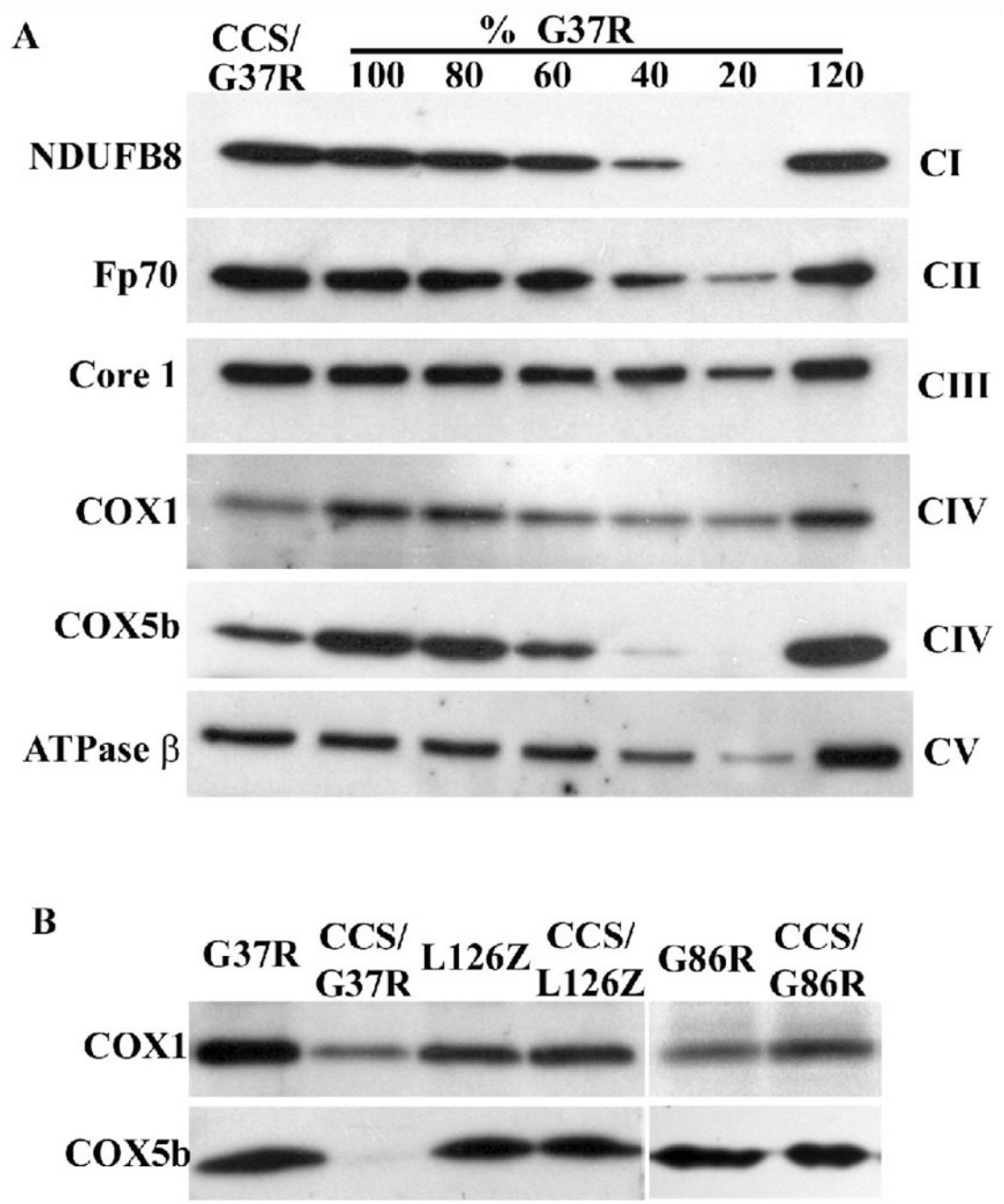

Fig. 3.

Analysis of mitochondrial OXPHOS complex subunit levels in mouse spinal cords. A. Mitochondrially enriched fractions of spinal cords from three week old CCS/G37R SOD1 and G37R SOD1 mice analyzed by SDS-PAGE and probed with antibodies specific for subunits of the various mitochondrial complexes. 20μg of protein for the CCS/G37R SOD1 sample was loaded. Concentration series of 20, 16, 12, 8, 4 and 24μg of G37R SOD1 protein sample was loaded for quantification control. CCS/G93A SOD1 spinal cord shows marked reductions in levels of complex IV subunits, COX1 and COX5b with no appreciable change in the other subunits. Filters were probed for subunits NDUFB8 (complex I), Fp70 (complex II), Core 1 (complex III), COX1 and COX5b (complex IV), or ATPase β (complex V). B. Mitochondrially

enriched fractions of spinal cords from three week old G37R SOD1, CCS/G37R SOD1, L126Z SOD1, CCS/L126Z SOD1, G86R SOD1 and CCS/G86R SOD1 mice analyzed by SDS-PAGE and probed with antibodies specific for complex IV subunits COX1 and COX5b. 20μg of protein was loaded per lane. CCS/126Z SOD1 and CCS/G86R SOD1 samples show no reduction in complex IV subunit levels compared to the single transgenics.

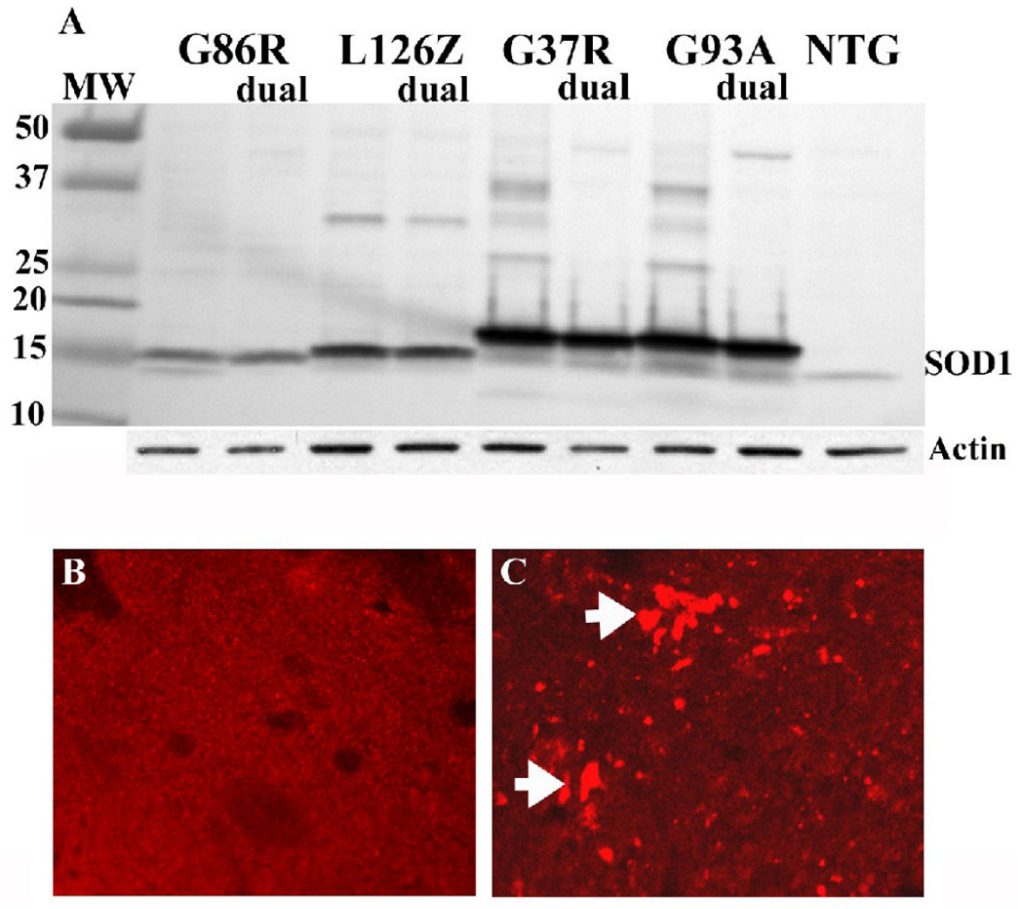

Fig. 4.

SOD1 aggregation is not accelerated with CCS over-expression.

A. Western blot of spinal cord extracts from paralyzed mice: 4 month old G86R SOD1 and 4 month old CCS/G86RSOD1 (dual); 8 month old L126Z SOD1 and 8 month old CCS/L126Z SOD1 (dual); 9 month old G37R SOD1 and 32 day old CCS/G37R SOD1 (dual); 8 month old G93A SOD1 and 23 day old CCS/G93A SOD1 (dual), or non-transgenic mouse (NTG). The samples were analyzed by 4-20% SDS-PAGE, and probed for SOD1 and actin (used as a loading control). 20 μg of protein was loaded per lane. SOD1 positive HMWPCs are not observed in weak CCS/G37R SOD1 or CCS/G93A SOD1 mice. End-stage G93ASOD1 and G37R SOD1 mice spinal cord homogenates demonstrate prominent SOD1 positive HMWPCs. Over-expression of CCS does not change the pattern/intensity of SOD1 positive bands in G86R SOD1 or L126Z SOD1 mice. MW = molecular weight standards. B. Ubiquitin immuno-fluorescence of spinal cord ventral horn sections of weak 23 day old CCS/G37R SOD1 and 8 month G37R SOD1 mice. Arrowheads highlight prominent ubiquitin positive inclusions observed only in weak G37R SOD1 mice but not weak CCS/G37R SOD1 mice. Magnification = 200×.

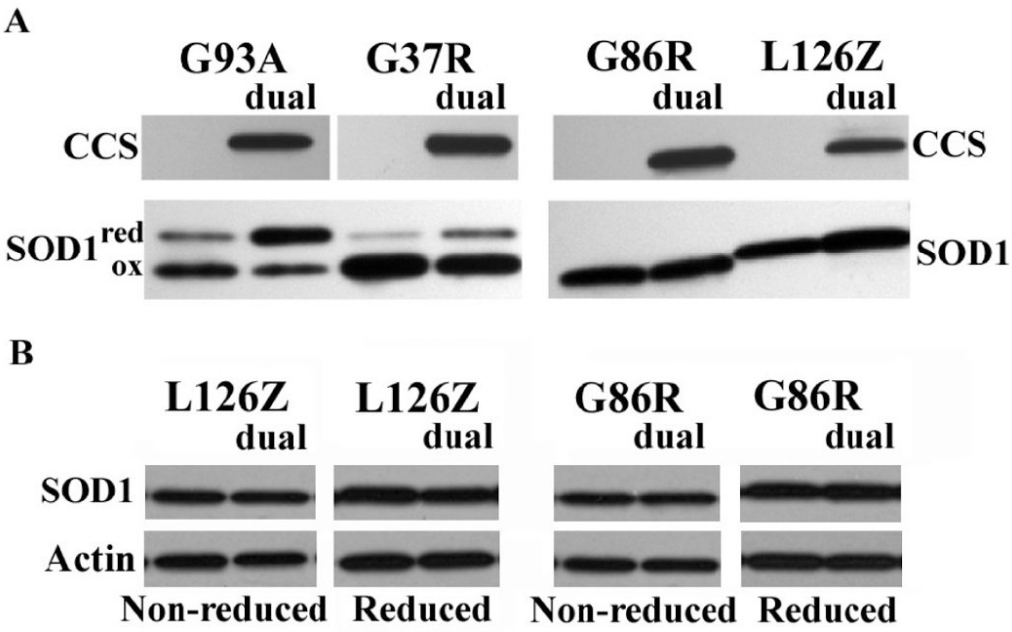

Fig. 5.

Effect of CCS over-expression on SOD1 disulfide reduction in spinal cords. Spinal cord homogenates were prepared in the presence of IAM. A. Samples, which were not treated with reducing agents or boiled, derived from G93A SOD1, CCS/G93A SOD1, G37R SOD1, CCS/G37R SOD1, G86R SOD1, CCS/G86R SOD1, L126Z SOD1 and CCS/L126Z SOD1 spinal cords. B. Both non-treated and beta-mercaptoethanol treated, boiled samples from L126Z SOD1 and CCS/L126Z SOD1, or 86R SOD1 and CCS/G86R SOD1 spinal cords. Samples were analyzed by 15% SDS –PAGE. 1.5 μg of protein was loaded per lane and probed for SOD1, CCS and actin. G93A SOD1 and G37R SOD1 exist in both oxidized and reduced forms, and CCS over-expression tends to increase the proportion of the reduced form. L126Z SOD1 and G86R SOD1 are detected in a single reduced form either in the presence or absence of CCS over-expression.